Surface Patterns on Subliming and Liquefying Ablation Materials

Hans W. Stock*
von Karman Institute for Fluiddynamics, Rhode Saint Genese, Belgium

The cross-hatching phenomenon has been studied experimentally at a freestream Mach number of 5.3, using two different low temperature ablation materials, camphor and wax, which sublime and liquefy, respectively, under the test conditions. The surface pattern parameters (i.e., the cant angle and the streamwise spacing) have been compared for both ablation modes and correlated with flowfield properties. The effect of exposure time under ablation conditions has been studied. It has been qualitatively shown that the viscosity of the solid ablation material influences the streamwise spacing. Streamwise vortices which occasionally develop in the boundary layer have no influence on the pattern formation.

I. Introduction

THE heating rates during earth atmosphere re-entry are such that an effective thermal protection is required. Among the possible techniques, ablation has proven to be satisfactory in high-heating conditions for both short and long duration re-entry trajectories.[1] It has been observed on recovered, slender re-entry vehicles, that regular patterns were generated on the surface of the ablation material. Similar phenomena were seen in the course of wind-tunnel tests on low-temperature ablation models. These surface patterns can be classified in three different types: streamwise grooves, turbulent wedges, and cross-hatching (Fig. 1).

Streamwise grooves[2-5] are believed to be created by streamwise vortices situated in the boundary layer which locally increase heat and mass transfer rates. The vortices have been shown to exist in supersonic laminar, transitional, and turbulent boundary layers, for instance downstream of backward facing steps[6] and also on concave surfaces. In wind-tunnel tests, backward facing steps naturally develop by ablation just downstream of a nonablating nose, Fig. 1, and concave surfaces are formed in the transition region due to increased mass transfer rates. Turbulent wedges have been investigated in Refs. 7-10. In these experiments local areas of turbulent boundary layer flow, in which turbulence is triggered by surface roughnesses, are imbedded into a laminar boundary layer. The lateral spreading of turbulence produces wedge-shaped regions, in which the mass transfer rates are increased. The third type of surface patterns is cross-hatching. It consists of two families of nearly straight grooves of regular spacing, running obliquely to the flow direction outside the boundary layer, producing a highly ordered pattern[2-5,9,11-16].

In this paper experimental results are presented which extend those in Refs. 12 and 13. A complete test program on the subliming ablator, camphor, was undertaken. Thus, a comparison of the results obtained on liquefying and subliming materials is possible.

II. Experimental Techniques

The experimental program was carried out in the same facility and under similar flow conditions as in Refs. 12 and 13. The dimensions of the models are given in Table 1. The ablation materials were wax and camphor which liquefy and sublime, respectively, under the present test conditions.

Received September 12, 1974; revision received February 18, 1975.
Index categories: Supersonic and Hypersonic Flow; Material Ablation.

*Research assistant; presently with Dornier GmbH, Friedrichshafen, Germany. The author would like to thank Prof. J. J. Ginoux, Head of the VKI Department of Supersonic and Hypersonics, for his continuous help and encouragement.

III. Test Results and Discussion

Transitional or Turbulent Boundary-Layer Flow

Although no systematic experimental evidence was available, it has been stated in the literature[2,3] that cross-hatching has never been observed in regions where the boundary layer was laminar. This condition was carefully tested and analyzed in the present study.

In Fig. 2, the Reynolds number Re_x, where x is the distance from the apex of cones to the location at which the cross-hatched pattern started, has been plotted against the Mach number at the outer edge of the boundary layer. Figure 2 also shows the transition Reynolds number for smooth cones[17-20] and demonstrates that the boundary layer is at least transitional in the region where the cross-hatched pattern starts to develop. An additional result which relates the onset of cross-hatching with boundary-layer transition is given in Fig. 3, which shows photographs of camphor models of the same geometry tested at the same stagnation pressure but at different stagnation temperatures. As can be seen, the onset of the cross-hatched pattern moves downstream as the stagnation temperature rises and thereby the Reynolds number Re_e is decreased. Another example is given in Fig. 1. The photograph in the middle shows turbulent wedges on a self-blunting cone. Cross-hatching appears only inside the turbulent wedges and not outside, where the boundary layer is still laminar.

Cross-Hatching Pattern Parameters

From experimental observations, correlations have been established between the flowfield conditions and the pattern parameters, i.e., the streamwise spacing and the cant angle.

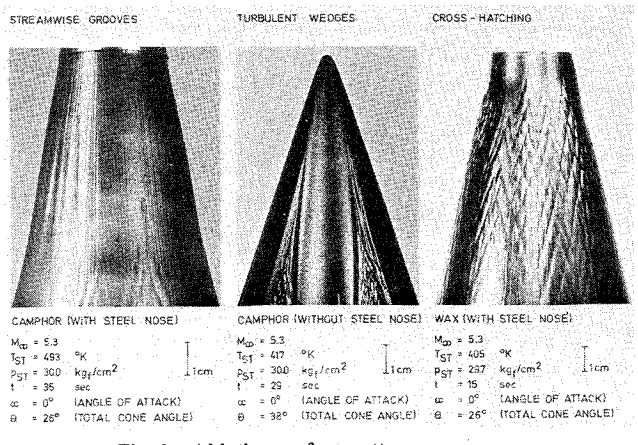

Fig. 1 Ablation surface patterns on cones.

Table 1 Cone and cone-flare dimensions

CONE DIMENSIONS:

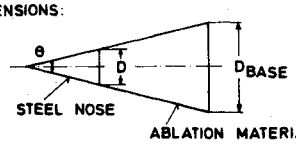

θ deg	D mm*	D_{BASE} mm*	θ deg	D mm*	D_{BASE} mm*	θ deg	D mm*	D_{BASE} mm*
10	20,45	80	24	30	80	42	20	70
12	32	80	26	33	80	46	20	60
14	32	80	28	35	80	50	20	60
16	32	80	30	38	80	54	20	50
18	32	80	34	20	70	58	22	50
20	26	80	38	20	70	62	22	50
22	28	80	40	18	70			

CONE-FLARE DIMENSIONS:

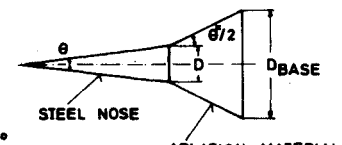

θ = 10°
D = 45 mm*
D_{BASE} = 80 mm*
θ* = 12-40° IN STEPS OF 2°

Cant angle

The cant angle ϕ is plotted vs the local Mach number M_e in Fig. 4. Available wind-tunnel data and free-flight data[3] are shown for comparison. As seen, the present results follow the Mach angle trend in the Mach number range 2.5-5.0 for both types of ablation materials. On the other hand, the flight data of Ref. 3 do not correlate with the Mach angle law. A possible explanation for such a discrepancy is that the cone Mach number at the location, where the cant angle was measured, was rather indeterminate due to nose blunting occuring in free-flight tests. This is demonstrated in Fig. 5 which shows the cant angle ϕ measured on self-blunting cones plotted against the Mach number M_e calculated for sharp nose cones and compared with present data from Fig. 4 and free-flight data.[3] (The blunted cone data are given in Table 2).

An approximate method[21] has been used to calculate the Mach number distribution on spherically blunted cones. Figure 6 shows the cant angle ϕ plotted vs the Mach number M_e, calculated either for sharp nose cones or with the method of Ref. 21. As may be seen, the data for wax and camphor based on the true local Mach number lie below the Mach angle line (solid curve) instead of above as in Fig. 4. This difference stems from the fact that the nose radius is not exactly known at the very moment when cross-hatching is formed. Thus M_e is underestimated, since the calculations are based on a nose radius which was measured after a run time, when the pattern

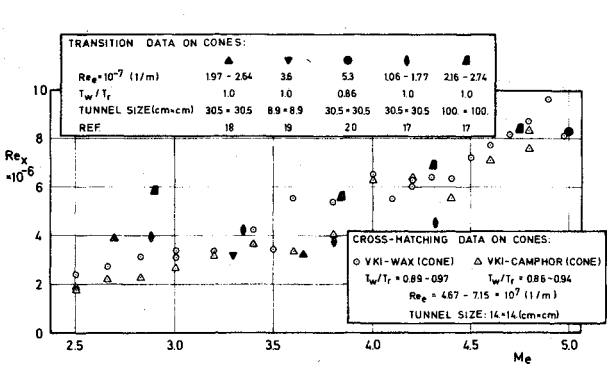

Fig. 2 Local Reynolds number evaluated at the position of transition and of the start of the cross-hatched pattern vs Mach number.

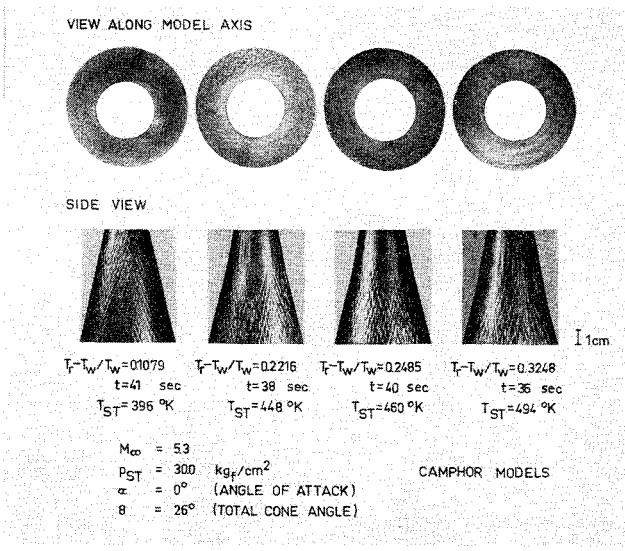

Fig. 3 The cross-hatched pattern on camphor models, tested at different stagnation temperatures.

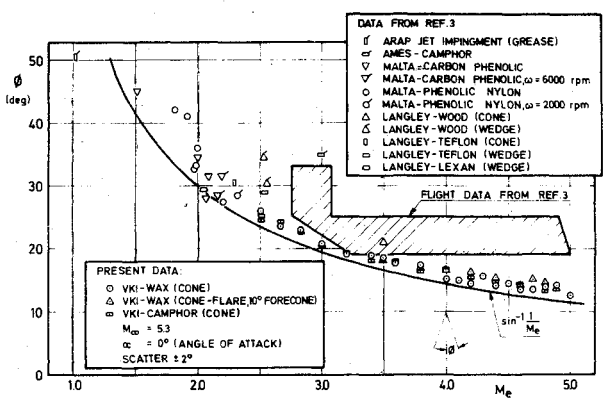

Fig. 4 Variation of the cant angle ϕ with the Mach number M_e.

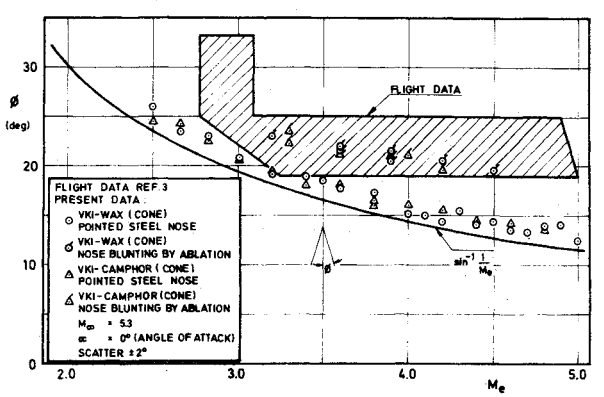

Fig. 5 Cant angle ϕ vs Mach number M_e.

was fully developed. Figure 6 also shows that the camphor test results differ even more from the Mach angle law than the wax data which may be explained by the fact that the nose radius-run time dependence is different for each ablation material.

The cant angle was seen to depend for the present tests uniquely on the local Mach number. It was found that the unit freestream Reynolds number Re_∞, the Reynolds number based on conditions at the outer edge of the boundary layer Re_e, the static pressure p_e, the driving temperature ratio, $(T_r - T_w)/T_w$, the run time, the ablation mode, and the material

Table 2 Dimensions and cross-hatching data of self-blunted cones

SELF-BLUNTED CONES:

DIMENSIONS AND CROSS-HATCHING DATA

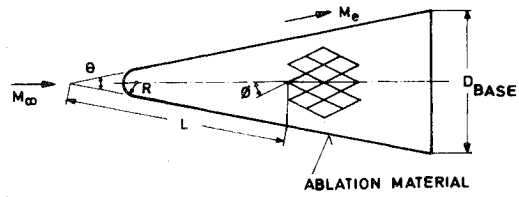

M_e: MACH-NUMBER AT THE OUTER EDGE OF THE BOUNDARY LAYER CALCULATED FOR POINTED NOSE CONES

	θ deg	M_e -	ø deg	R mm	L mm	D_{BASE} mm ø
WAX	20	4.5	19.5	3.8	180	80
	26	4.2	20.5	4.0	150	80
	32	3.9	20.5, 21.5	3.3	120	70
	38	3.6	21.5, 22.0	2.5	85	70
	46	3.2	23.0	2.5	60	60
CAMPHOR	26	4.2	19.5	5.0	90	80
	30	4.0	21.0	5.0	130	80
	32	3.9	21.0	5.3	100	70
	38	3.6	21.5	5.0	80	70
	44	3.3	22.3, 23.5	4.0	50	60

properties had no influence on ϕ. The cant angle did not vary in the downstream direction. (The recovery temperature T_r was calculated by assuming a turbulent recovery factor of 0.895. The wall temperature $T_w = 337$ K, is the temperature at which wax liquefies independently of p_e. For the camphor tests T_w is dependent on p_e, the heat transfer rate, and thereby the mass transfer. In Ref. 16 a method is described to calculate T_w for subliming materials in the presence of a turbulent boundary layer.)

Streamwise spacing

The effect of the surface pressure p_e on λ is shown in Fig. 7. The results agree quite well with those of Williams,[4] extending the range to lower static pressures and greater values of λ. The surface pressure p_e was varied both by changing the cone or flare angle and by occasionally altering the tunnel stagnation pressure. Figure 8 demonstrates that nose blunting has no influence on λ contrary to its effect on the cant angle ϕ. The static pressure p_e rapidly approaches (close to the junction sphere-cone) the sharp cone value, as opposed to the slow trend of the Mach number M_e[21].

The effect of the driving temperature ratio $(T_r - T_w)/T_w$ on the streamwise spacing is shown in Fig. 9 for constant

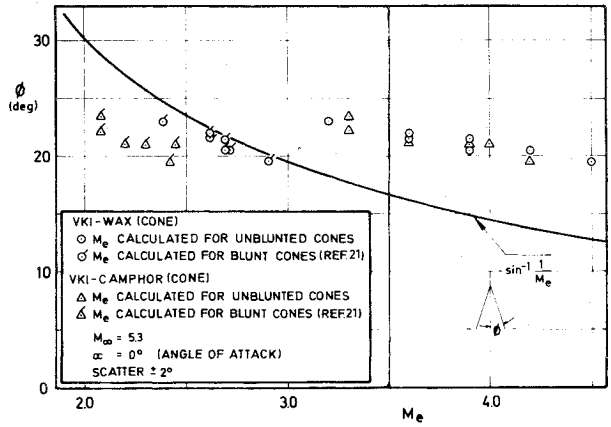

Fig. 6 Cant angle ϕ vs Mach number M_e, measured on self-blunting cones.

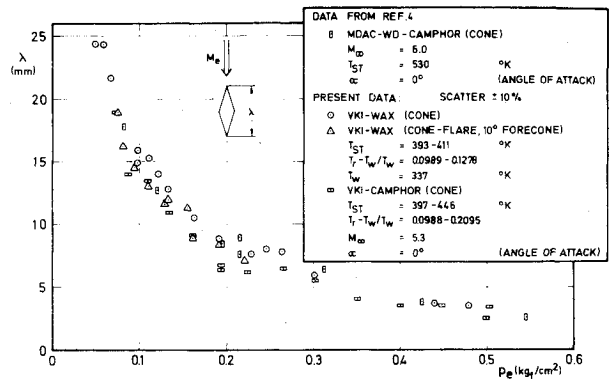

Fig. 7 The dependence of the streamwise spacing λ on the local static pressure p_e.

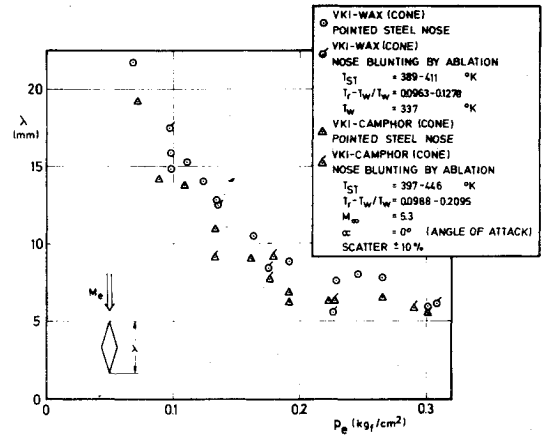

Fig. 8 Streamwise spacing λ vs the local static pressure p_e, including data on self-blunting cones.

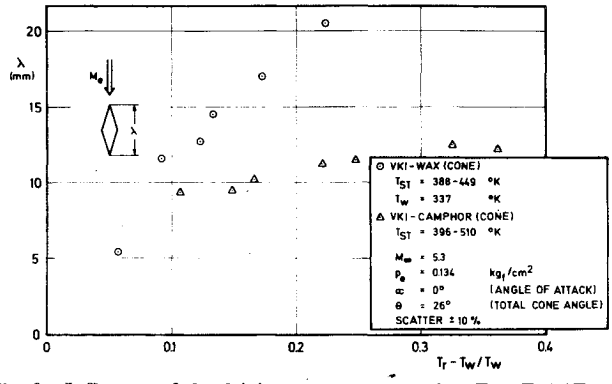

Fig. 9 Influence of the driving temperature ratio $(T_r - T_w)/T_w$ on the streamwise spacing λ.

values of p_e. λ is strongly dependent on $(T_r - T_w)/T_w$ for wax tests, whereas for camphor λ increases only slightly with the driving temperature. Figure 3 shows photographs of camphor models tested at different values of $(T_r - T_w)/T_w$.

The Mach number M_e, the Reynolds numbers Re_∞ and Re_e, and the run time did not appear to have any influence on λ, when the static pressure p_e and the driving temperature ratio were held constant. No influence of nose blunting on λ could be observed. The body size did not seem to be a scaling factor for λ. Indeed, Williams[4] used camphor models which were three times larger than those tested at VKI and no difference in λ could be seen (Fig. 7). The streamwise spacing increased slightly in the downstream direction.

Run Time

Figure 10 shows photographs of the cross-hatching development reproduced from a movie taken during a test.

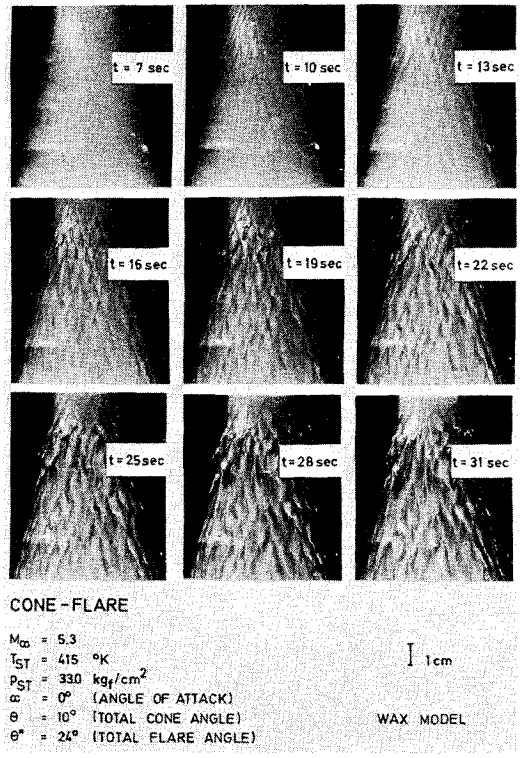

Fig. 10 Influence of the run time on the cross-hatching development.

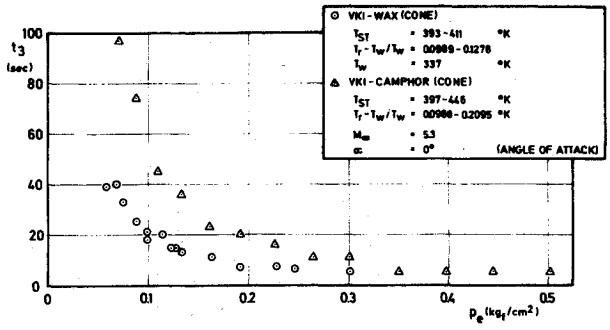

Fig. 11 Run time required for a developed cross-hatched pattern as a function of the local static pressure p_e.

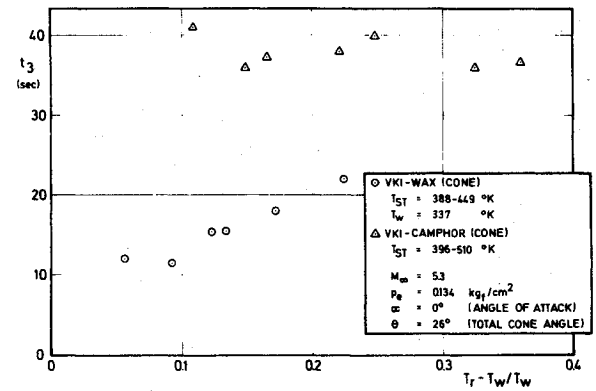

Fig. 12 Run time required for a developed cross-hatched pattern as a function of the driving temperature ratio $(T_r - T_w)/T_w$.

Several distinct time intervals can be defined corresponding to different stages in the development of the cross-hatched pattern:

1st time interval: $t_0 - t_1$. From tunnel start until the model surface reaches the liquefaction or sublimation temperature and starts to ablate.

2nd time interval: $t_1 - t_2$. From the onset of ablation until cross-hatching starts to appear.

3rd time interval: $t_2 - t_3$. From the first visible evidence of cross-hatching until the surface pattern is fully developed, showing the maximum height difference between the bottom of the grooves and the enclosed hills.

4th time interval: t_3- . After being fully developed, the pattern starts to disintegrate, showing a regmaglypt pattern resembling those on meteorites shown in Ref. 2.

In the test shown in Fig. 10, cross-hatching started to appear at $t_2 = 7$ sec and was fully developed at $t_3 = 13$-16 sec. The long run time photos show the pattern disintegration process. As may be seen during the time period t_2 until t_3, the cant angle ϕ and the streamwise spacing λ were independent of time.

It was found that the run time t_3 for both camphor and wax models was dependent on the local static pressure p_e (Fig. 11). t_3 decreased with increasing static pressure p_e and was roughly twice as long for camphor models for the same p_e. In Fig. 12, t_3 is shown as a function of the driving temperature ratio $(T_r - T_w)/T_w$ for constant Pe. t_3 increases nearly linearly with $(T_r - T_w)/T_w$ for wax, while for camphor t_3 remains constant.

Angle of Attack

Figure 13 gives the test results on cones at angle of attack from 0-6° at 2° intervals. As the maximum pressure was obtained on the windward side of the model, the tunnel was stopped when a marked pattern was seen there. The run time decreased with increasing angle of attack, i.e., increasing windward side static pressure, leading to a gradual vanishing of the pattern on the leeward side.

On the model sides, the pattern became progressively more inclined relatively to the side meridian, as the angle of attack was increased. (The pattern inclination or orientation is defined by the direction of the bisectrix of the angle between left and right running grooves). The inclination angle of the pattern was measured on the model sides and is plotted vs the angle of attack in Fig. 14. The streamline inclination calculated by a method of characteristics applied to slender bodies[5] is shown for comparison. As may be seen, the pattern orientation is very close to the streamline direction of the inviscid flow. A similar observation is qualitatively described in Ref. 3. On ablating cones spinning at 2000 and 6000 rpm, the cross-hatched pattern was shifted in a direction which was consistent with the local cross flow.

Influence of the Viscosity of the Solid Ablation Material on the Streamwise Spacing

On wax models, keeping all conditions constant, it was shown that λ increased from 5-20 mm for only small changes in the stagnation temperature (60 K) (Fig. 9). On the other hand, a change in the stagnation temperature of 120 K for the camphor tests had virtually no effect on the streamwise spacing.

The cross-hatching phenomenon results from an interaction between the boundary layer and the solid ablation material. It is reasonable to assume that the boundary layer is not significantly modified by the changes in the heat transfer. Consequently, some properties of the ablation material must behave differently under small changes in heat transfer rate, i.e., temperature. The physical property of wax which is very sensitive to a small temperature change is its viscosity

$$\mu = GT = (E/2)\,T \qquad (1)$$

It is shown in Ref. 16 that both materials, wax and camphor, are visco-elastic solids of the Maxwell type. The experimental determination of the elasticity modulus E and the relaxation time T for wax and camphor, is described in Ref. 16. The results are given in Figs. 15 and 16. Figure 15 shows that E_{wax} decreases drastically from 150-2 Kg_f/cm^2 during a temperature rise from 295-323 K, which corresponds to the ex-

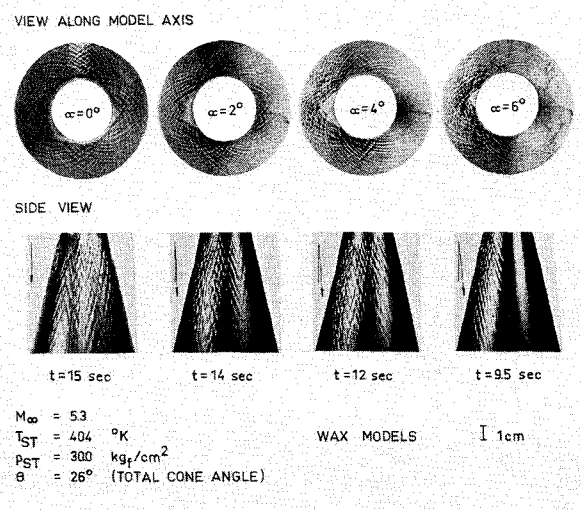

Fig. 13 Influence of the angle of attack on cross-hatching.

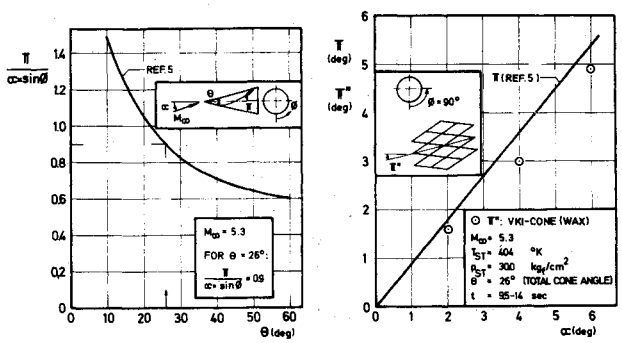

Fig. 14 Comparison of the pattern inclination angle π^* with the streamline inclination angle π of the inviscid flow for cones at angle of attack on the model side ($\phi = 90°$).

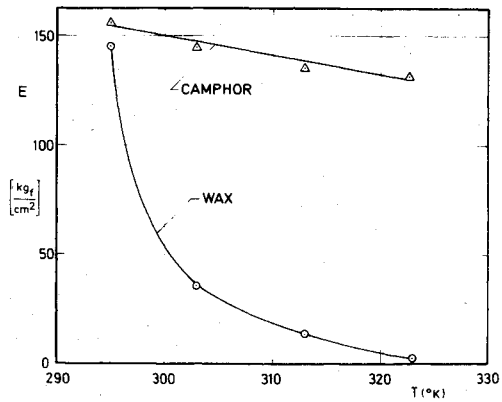

Fig. 15 Variation of the elasticity modulus E with material temperature.

pected temperature variation of the solid wax during a test (293 K is the initial temperature before the tests and 337 K is the liquefaction temperature of wax). In the same range of material temperature, E_{camphor} changes only slightly (293 K initial temperature, 344 K maximum wall temperature). Furthermore it is shown in Fig. 16 that the relaxation time T decreases considerably with temperature for wax but not for camphor, hence only the viscosity of the wax (see Eq. 1) is a highly dependent function of the temperature.

It has now to be demonstrated that the streamwise spacing λ varies with the viscosity of the solid wax, based on the information of Figs. 9, 15 and 16. The temperature distribution in the solid wax for the actual test cases has been calculated

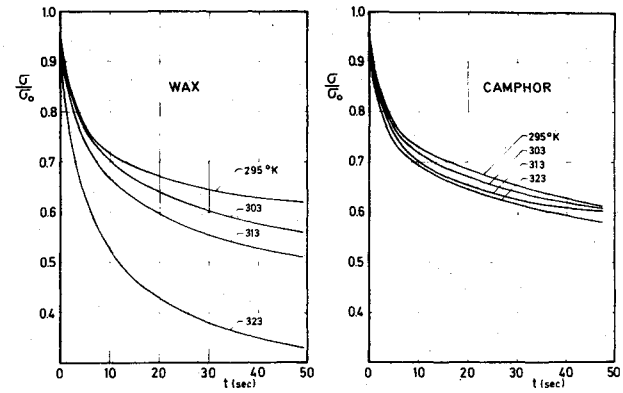

Fig. 16 Stress variation with time for constant strain at different material temperatures.

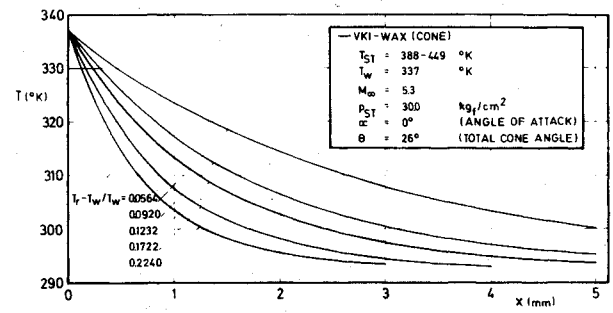

Fig. 17 Temperature distribution in the solid wax at different driving temperature ratios $(T_r - T_w)/T_w$.

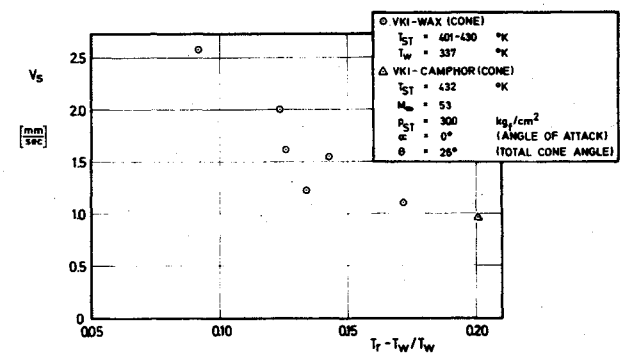

Fig. 18 Propagation speed of the cross-hatched pattern V_s vs the driving temperature ratio.

using the method of Ref. 22, which is valid for steady-state ablation conditions. In Ref. 16 it is shown that indeed cross-hatching starts to develop after a run time when steady-state conditions have been achieved. The calculated temperature distribution is shown in Fig. 17; the liquid-solid interface is at $x = 0$. As the material close to the interface gets colder for increasing $(T_r - T_w)/T_w$, the viscosity of the solid wax increases rapidly (Figs. 15 and 16). It is thus shown that the streamwise spacing λ decreases if the viscosity of the solid material in the layer, which is affected by the ablation process, gets smaller.

In Ref. 13 it was seen that λ increased for the same model geometry and test conditions if the ablation material was preheated prior to the run. This discrepancy to the present findings is because of the following: The preheating was such that all the ablation material was at a high temperature whereas in the test cases described previously only a thin layer of the material below the liquid-solid interface was affected by the heat transfer during the run and all the model interior remained cold.

Figure 18 shows an experimental result which proves that viscosity of wax changes with the driving temperature. In the

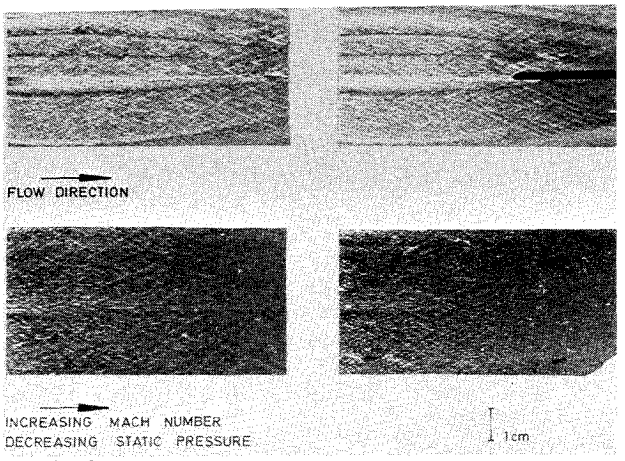

Fig. 19 Oil film surface patterns on the wall in the expansion region of a Mach 3.5 nozzle.

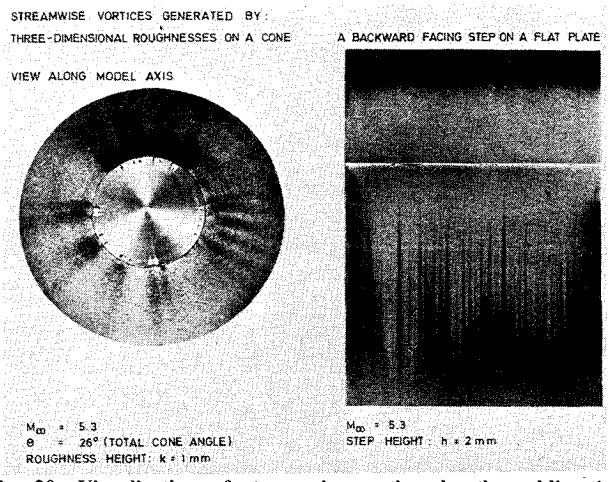

Fig. 20 Visualization of streamwise vortices by the sublimation technique.

course of a few runs with wax and camphor cones of the same apex angle, tested at the same static pressure p_e but at different driving temperature ratios, a film was taken during the complete testing period. This showed that the whole cross-hatched pattern moved very slowly downstream. Furthermore, it was verified that the velocity of propagation was a function of the driving temperature. The result is shown in Fig. 18, which indicates that this velocity decreases nearly linearly with $(T_r - T_w)/T_w$ for wax. The shear stress acting on the solid, which is transmitted from the gas via the liquid film, does not change significantly with $(T_r - T_w)/T_w$. Hence, the difference in the propagation velocity V_s is due to the change in the viscosity of the solid.

Probstein and Gold[23] suggested a triggering mechanism for cross-hatching which is based on an interaction between the shear stress fluctuations in a turbulent boundary layer at the wall and the deformation of a viscous solid. The behavior of such a solid is described by its relaxation time and shear or elasticity modulus. The experimental findings thus support the hypothesis used in the calculations of Refs. 23-26. Furthermore, no ablative mass transfer is necessary in this model for the formation of cross-hatching. This is supported by some experimental results which are shown in Fig. 19 (similar observations are given in Ref. 27). In the present case, the cross-hatched pattern is produced on the surface of an oil film containing magnesium oxide spreading over a glass window in the expansion part of a supersonic nozzle under the effect of friction. The vapor pressure of the highly viscous oil was well below the static pressure level in the tunnel, and consequently, there was no ablation mass transfer. A close inspection of the

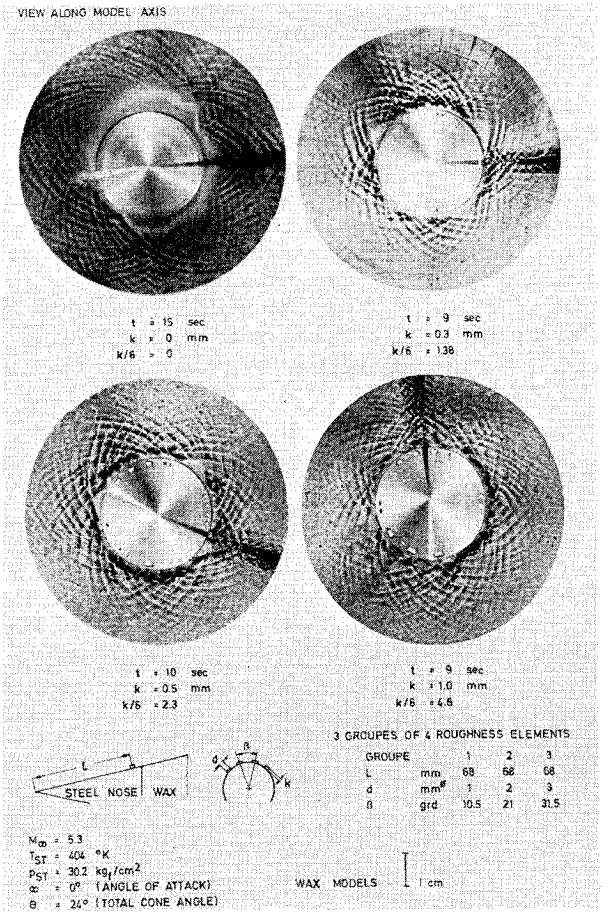

Fig. 21 Influence of three-dimensional roughnesses on the cross-hatching formation.

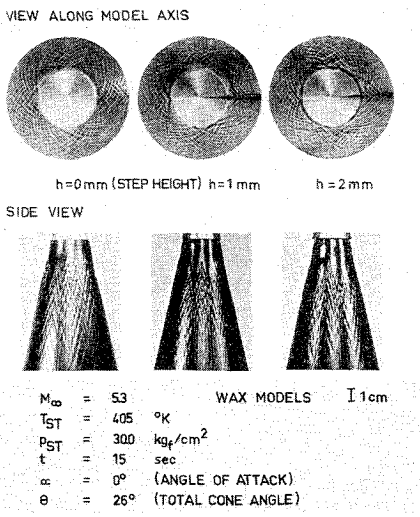

Fig. 22 Influence of a backward facing step on the cross-hatching formation.

figure shows all the features of conventionally obtained cross-hatched patterns. The streamwise spacing λ increases and the cant angle ϕ decreases in the flow direction as the static pressure falls and the Mach number rises.

Streamwise Vortices and Cross-Hatching

Tobak[28] assumed that streamwise vortices, which occasionally develop in the boundary layer, are the cause for the cross-hatched pattern formation. In order to check Tobak's hypothesis, streamwise vortices were artifically created inside

the boundary layer by three-dimensional roughness elements and by backward facing steps. Figure 20 shows streamwise vortices visualized by the sublimation technique on nonablating models. Figure 21 gives the test results on ablating cones, on which three-dimensional roughness elements of different height, diameter, and spacing were installed to produce vortices of different intensity and spacing.[29] Although the tests were done over a considerable range of roughness geometry parameters, the pattern remained essentially unchanged. Figure 22 shows the results on ablating cones involving backward facing steps of different heights. Here again cross-hatching is unchanged.

Hence, the following reasoning is used. If the existence of streamwise vortices is necessary for the generation of cross-hatching, the resulting pattern should be coupled in some way to its creating mechanism. Weak perturbations have been observed on some models due to ablation-induced backward facing steps and surface concavities. Now, the perturbations artificially introduced create vortices of much larger strength and different spacing. But, as mentioned previously, they have no observed effect on the pattern formation. Hence, streamwise vortices are not believed to be necessary for cross-hatching to exist.

IV. Conclusions

1) It is shown that a necessary condition for the existence of cross-hatching is that the boundary layer should be transitional or turbulent. 2) The cant angle ϕ is for the present tests a unique function of the local Mach number outside the boundary layer and is nearly equal to the local Mach angle even on self-blunting cones for both subliming and liquefying ablation materials. 3) The streamwise spacing λ is inversely proportional to the local static pressure p_e and increases slightly in the downstream direction for both materials. λ increases with the driving temperature ratio $(T_r - T_w)/T_w$ for wax and stays nearly constant for camphor. 4) The run time t_3 necessary to form the cross-hatched pattern is inversely proportional to the local static pressure p_e for wax and camphor. t_3 increases with the driving temperature ratio $(T_r - T_w)/T_w$ for wax and stays nearly constant for camphor. 5) The pattern orientation is closely linked to the streamline direction in the inviscid flow. 6) The streamwise spacing λ increases as the viscosity of the solid ablation material increases. 7) The cross-hatched pattern propagates slowly in the downstream direction at a speed which increases as the viscosity of the solid ablation material is decreased. 8) Cross-hatching is also formed in the absence of any ablative mass transfer. 9) The presence of streamwise vortices in the boundary layer does not seem to be necessary to trigger cross-hatching.

References

[1] Scala, S. M., "The Thermal Protection of a Re-entry Satellite," *American Rocket Society Journal*, Vol. 29, Sept. 1959, p. 670-672.

[2] Larson, H. K. and Mateer, G. G., "Cross-Hatching—A Coupling of Gas Dynamics with the Ablation Process," AIAA Paper 68-670, Los Angeles, Calif., 1968.

[3] Laganelli, A. L. and Nestler, D. E., "Surface Ablation Patterns: A Phenomenology Study," *AIAA Journal*, Vol. 7, July 1969, pp. 1319-1325.

[4] Williams, E. P., "Experimental Studies of Ablation Surface Patterns and Resulting Roll Torques," *AIAA Journal*, Vol. 9, July 1971, pp. 1315-1321.

[5] Mc. Devitt, J. B. and Mellenthin, J. A., "Upwash Patterns on Ablating and Nonablating Cones at Hypersonic Speeds," TN D 5346, May 1969, NASA.

[6] Ginoux, J. J., "The Existence of Three-Dimensional Perturbations in the Reattachment Region of a Two-Dimensional Supersonic Boundary Layer after Separation," AGARD R 272, April 1960.

[7] Canning, T. N., Tauber, M. E., and Wilkins, M. E., "Orderly Three-Dimensional Processes in Turbulent Boundary Layers on Ablating Bodies," AGARD CP 30, May 1968.

[8] Canning, T. N., Wilkins, M. E., and Tauber, M. E., "Ablation Patterns on Cones Having Laminar and Turbulent Flows," *AIAA Journal*, Vol. 6, Jan. 1968, pp. 174-175.

[9] Mc. Devitt, J. B., "An Exploratory Study of the Roll Behavior of Ablating Cones," *Journal of Spacecraft and Rockets*, Vol. 8, Feb. 1971, pp. 161-169.

[10] Wilkins, M. E., "Evidence of Surface Waves and Spreading of Turbulence on Ablating Models, *AIAA Journal*, Vol. 3, Oct. 1965, pp. 1963-1965.

[11] Canning, T. N., Wilkins, M. E., and Tauber, M. E., "Boundary Layer Phenomena Observed on the Ablated Surface on Cones Recovered after Flights at Speeds up to 7km/sec.," AGARD CP 19, Vol. 2, May 1967.

[12] Stock, H. W. and Ginoux, J. J., "Experimental Results on Cross-Hatched Ablation Patterns," *AIAA Journal*, Vol. 9, May 1971, pp. 971-973.

[13] Stock, H. W. and Ginoux, J. J., "Further Experimental Studies of Cross-Hatching," *AIAA Journal*, Vol. 10, April 1972, pp. 557-558.

[14] Langanelli, A. L. and Zempel, R. E., "Observations of Surface Ablation Patterns in Subliming Materials," *AIAA Journal*, Vol. 8, Sept. 1970, pp. 1709-1711.

[15] Nachtsheim, P. R. and Larson, H. K., "Cross-Hatched Ablation Patterns in Teflon," *AIAA Journal*, Vol. 9, Aug. 1971, pp. 1608-1614.

[16] Stock, H. W. and Godard, M., "Cross-Hatching: A Comparison between the Behavior of Liquefying and Subliming Ablation Materials," TN 85, April 1973, von Karman Institute for Fluid Dynamics, Rhode Saint Genese, Belgium.

[17] Pate, S. R., "Measurements and Correlations of Transition Reynolds Numbers on Sharp Slender Cones at High Speeds," TR 69-172, Dec. 1969, Arnold Engineering Development Center, Tullahoma, Tenn.

[18] Van Driest, E. R., and Boison, J. C., "Experiments on Boundary Layer Transition at Supersonic Speeds," *Journal of the Aerospace Sciences*, Vol. 24, Dec. 1957, pp. 885-899.

[19] Van Driest, E. R. and Boison, J. C., "Boundary Layer Stabilization by Surface Cooling in Supersonic Flow," *Journal of the Aerospace Sciences*, Vol. 22, Jan. 1955, p. 70-72.

[20] Potter, J. L. and Whitfield, J. D., "Boundary Layer Transition under Hypersonic Conditions," TR 65-99, May 1965, Arnold Engineering Development Center, Tullahoma, Tenn.

[21] Stock, H. W., "An Approximate Method to Calculate the Mach Number Distribution on Spherically Capped Cones at Zero Angle of Attack in Supersonic Flow," *Zeitschrift fuer Flugwissenschaften*, Vol. 22, Nov. 1974, pp. 372-379.

[22] Landau, H. G., "Heat Conduction in a Melting Solid," *Quarterly of Applied Mathematics*, Vol. 8, 1950, p. 81-94.

[23] Probstein, R. F. and Gold, H., "Cross-Hatching—A Material Response Phenomena," *AIAA Journal*, Vol. 8, Feb. 1970, pp. 364-366.

[24] Gold, H., Probstein, R. F., and Scullen, R., "Inelastic Deformation and Cross-Hatching," *AIAA Journal*, Vol. 9, Oct. 1971, pp. 1904-1910.

[25] Stock, H. W., "Role of the Anelastic Behavior of the Ablation Material on Cross-Hatching," *AIAA Journal*, Vol. 10, Nov. 1972, pp. 1528-1529; Errata *AIAA Journal*, Vol. 11, July 1973, pp. 1056.

[26] Stock, H. W., "Interaction between a High Speed Boundary Layer Flow and an Anelastic Deformable Solid Wall," TN 86, May 1973, von Karman Institute for Fluid Dynamics, Rhode Saint Genese, Belgium.

[27] Nachtsheim, P. R. and Hagen, J. R., "Observations of Cross-hatched Wave Patterns in Liquid Films, *AIAA Journal*, Vol. 10, Dec. 1972, pp. 1637-1640.

[28] Tobak, M., "Hypotheses for the Origin of Cross-Hatching," *AIAA Journal*, Vol. 8, Feb. 1970, pp. 330-334.

[29] Schnell, W. C. and Ginoux, J. J., "Effect of Surface Roughness on Axisymmetric Laminar Separated Flows at M 5.3," TN 41, Jan. 1968, von Karman Institute for Fluid Dynamics, Rhode Saint Genese, Belgium.